

Electrochemical investigation of copper oxide films formed by oxygen plasma treatment

N. BELLAKHAL, K. DRAOU, J. L. BRISSET*

Laboratoire d'Analyse Spectroscopique et de Traitement de Surface des Matériaux (Equipe LEICA), UFR des Sciences, 76821 Mont Saint Aignan Cedex, France

Received 16 January 1996; revised 1 July 1996

Linear potential sweep voltammetry was used to characterize the copper oxides grown on a metal substrate when exposed to a low pressure inductively coupled oxygen plasma. This study confirms the formation of a precursor oxide Cu_xO ($x > 4$), two copper(I) oxides Cu_{2-x}O and Cu_3O_2 and copper(II) oxide CuO . The electrochemical reduction curve of Cu_xO is characterized in aqueous solution (pH 9.2) by a minor peak near -0.5 V vs SCE while the two Cu(I) oxides present one reduction peak at -0.8 V vs SCE and cannot be electrochemically separated; CuO is reduced to Cu(I) at -0.65 V vs SCE. The reduction potentials of the copper(I) and copper(II) oxides vary with the oxide layer thickness which increases with the time of exposure to the plasma and the injected electric power and decreases as the distance between the sample and the 1st coil increases for given treatment parameters. In addition, a mechanism is proposed for the reduction of thin films containing the copper(I) and copper(II) oxides formed after plasma treatment.

1. Introduction

A plasma gas is characterized by the occurrence of a large number of excited species which confers on them an enhanced reactivity involved in numerous plasma treatments of materials. These chemical properties are classified in the usual way into acid–base properties (including Brønsted and Lewis acidities) and oxidation–reduction properties. The present work has focused on the latter which has been studied for air corona oxidation of liquids and aqueous solutes [1]. Particular plasmas, such as the corona discharges in natural air, also give rise to oxidation reactions at the treated materials. Thus, they were described as useful tools to simulate the corrosion of metallic materials and the ageing of polymers in natural conditions [2–4]; the relevant corrosion processes involve the water molecules present at the surface. This investigation was performed with an oxygen plasma gas produced by a classical 13.56 MHz inductively coupled plasma generator under reduced pressure.

In a plasma, a number of processes take place (e.g., ionization, dissociation by electron impact and attachment phenomena). These induce the formation of activated species such as, in the case of an oxygen plasma, excited molecules, atomic oxygen, ozone, molecular and atomic ions which are able to react at the metal surface and yield oxide layers. The literature [5, 6] reports the oxidizing properties of oxygen plasmas, and, for example, oxygen atoms are implied in the plasma treatment of YBaCuO thin films.

Copper forms several oxides. It was thus selected as an appropriate material to illustrate the oxidizing properties of an RF oxygen plasma and to quantify the influence of the discharge parameters (i.e., injected power, gas pressure, and distance between the treated sample and the first inductive coil). The choice of the metal was also governed by its universal use in the electrochemical industries and by the fact that oxides are often produced with electric discharges and breakdowns. Also, copper was previously selected for thermal oxidation studies [7–10], giving the opportunity to compare the respective efficiencies of plasma and thermal treatments.

The most popular techniques used to characterize the metal oxides are electrochemical methods [7, 8, 11] and, more recently, spectroscopy methods [9, 10]. For monitoring oxide films on copper in the wire industry, Pops and Mennessy [12] recommended a galvanostatic method, involving the cathodic reduction of oxide to metal. Deutscher and Woods [7] confirmed that electrochemical reduction can be useful for characterizing the oxide layers on copper. The formation and the reduction of oxide layers on copper electrodes during triangular potential sweeps in alkaline solution have also been studied [13, 14]; the reduction voltammograms show two peaks attributed to the reduction of the copper(II) and copper(I) oxides respectively produced during the oxidation sweep. In contrast to these observations, Pops and Hennessy [12] assigned the first peak to the reduction of Cu_2O and the second to that of CuO . Cathodic reduction of oxides formed on copper has also been described by Evans and Miley [15]. They suggest that the initial part of the potential–time

*Author to whom all correspondence should be addressed.

curve is related to the reduction to the Cu(I) oxide and the second part to that of the Cu(II) oxide. The reduction was considered to progress outward from the metal–oxide interface and, since Cu_2O is the favoured oxide in contact with copper metal, this species reacts first. Lenglet *et al.* [8] characterized the compounds grown on copper during thermal air oxidation performed at low temperature ($T < 573$ K) by linear potential sweep voltammetry and proposed a mechanism for the reduction of CuO and the non stoichiometric copper(I) oxide.

In this paper we report upon the electrochemical characterization of copper oxide films formed on a copper substrate by oxygen plasma treatment under various conditions. The oxides were previously identified by optical techniques such as photoluminescence spectroscopy. The nature and the characteristics of the oxide layer formed will be related to the working parameters of the oxygen plasma.

The basic key parameters to vary the plasma treatment conditions are the exposure duration, t , the injected electric power, P , and the distance, d , between the copper sample and the first coil. These parameters were varied and the formation of various

copper oxides observed in the same way as previously reported for thermal oxidation [9]. Another standard parameter used to characterize the plasma is the energy density P/N , where P refers to the electric power and N to the number of gas moles present in the plasma volume at pressure p and temperature $T_{\text{gas}} = 420$ K. The relevant volume is that of a cylinder defined by the radius r of the reactor and the length d between the first coil and the target ($\pi r^2 d$). N is given by $p\pi r^2 d/RT_{\text{gas}}$. Hence,

$$\frac{P}{N} = \frac{PRT_{\text{gas}}}{p\pi r^2 d}$$

2. Experimental details

2.1. Plasma device

The inductively coupled plasma reactor was a pyrex tube 10 cm in diameter and 30 cm in length connected to a primary pump and to the feeding gas device (Fig. 1). The oxygen plasma was created by a 13.56 MHz radio frequency generator coupled via a seven turn load coil through an impedance matching

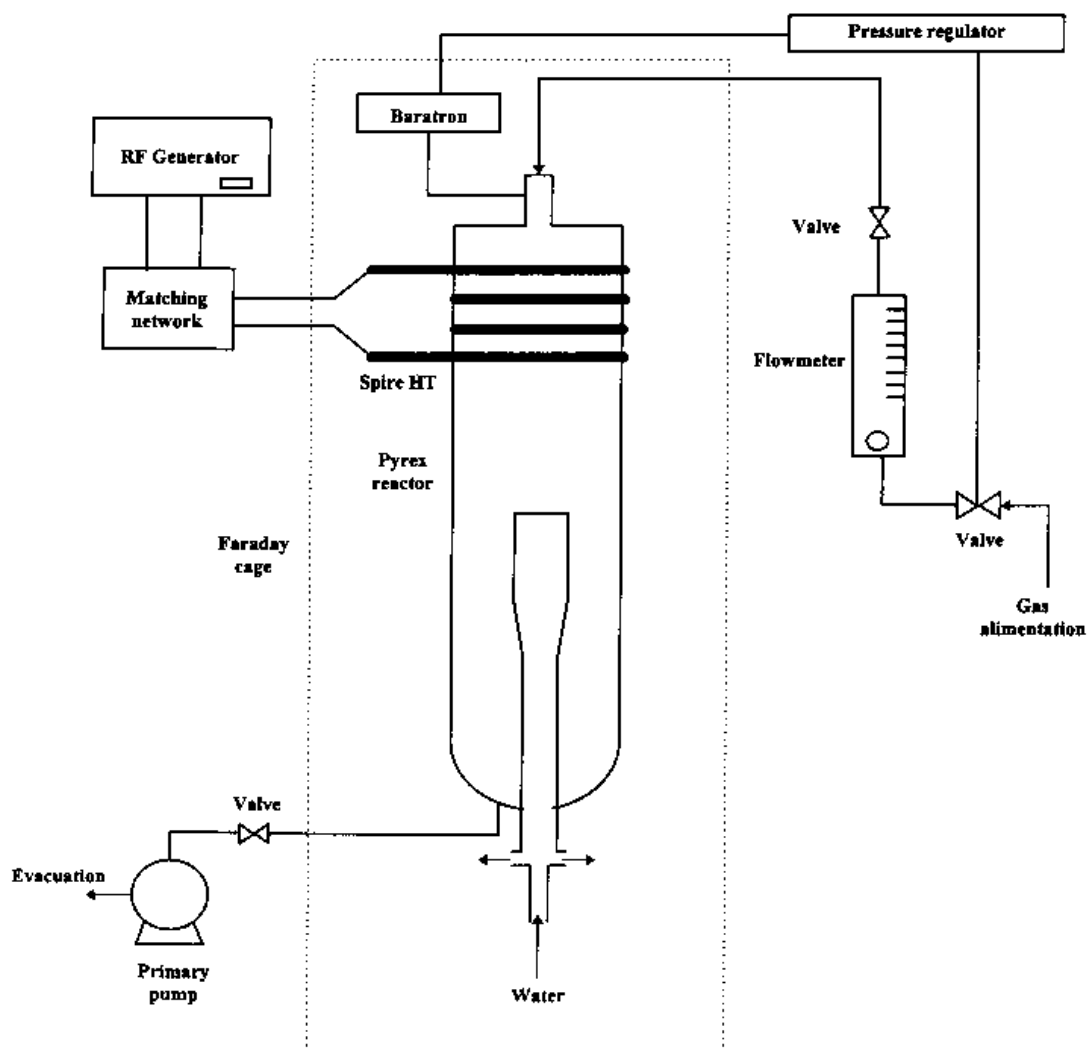


Fig. 1. Experimental setup.

Table 1. Chemical compositions of ETP copper*

Impurity/ppm	O	Ag	As	Pb	Fe	Ni	Sb	S	Se	Te
ETP copper	100	≤ 10	≤ 10	≤ 10	≤ 10	≤ 10	≤ 5	≤ 5		≤ 5

*For copper A, according to French nomenclature

network. The induced power was fixed in the range 100–2200 W. The copper foil sample was positioned normal to the gas flow ($0.25 \text{ dm}^3 \text{ min}^{-1}$) on a stainless steel quenching head cooled by water circulation. The vacuum (100–200 Pa) was sustained by a primary pump.

2.2. Starting material

The starting material was A-grade copper supplied by Alcatel–Cuivre which originally contained 100 ppm of oxygen in the form of Cu_2O . The chemical composition of the industrial starting metal is given in Table 1. The copper samples (0.3 mm thick foil with a surface area of 1.1 cm^2) were mechanically polished with different grinding papers (400, 800 and 1200 grade), washed in absolute ethanol and dried in a nitrogen flow before being exposed to the oxygen plasma.

2.3. Instrumental techniques

The electrochemical reduction curves were determined on a PAR 273 potentiostat associated with an IBM PC. The electrochemical cell was fitted with a platinum auxiliary electrode and the potentials measured with reference to a SCE. The selected electrolyte was a 0.1 M $\text{Na}_2\text{B}_4\text{O}_7$ solution, pH 9.2, as the solubilities of the various copper oxides and hydroxides are minimum at this pH. The potential sweep was fixed at 0.5 mVs^{-1} and before each run the electrolyte was carefully purged with nitrogen.

The luminescence spectra used to identify the copper(I) oxides were recorded with a Jobin–Yvon 3C spectrophotometer working in the 300–1200 nm range.

3. Results and discussion

3.1. Precursor oxide Cu_xO ($x > 4$)

A so called ‘precursor oxide’ Cu_xO ($x > 4$) was identified after a low temperature thermal treatment of copper (i.e., $T = 373 \text{ K}$, $t < 30 \text{ min}$) [10] but it is not mentioned as an air corrosion product [16–18]. Its crystallographic structure is similar to that of Cu_2O [9]. XPS and Auger analysis confirm the mixed valency character of copper (I–0) which is related to the scattering of interstitial Cu(0) in the Cu(I) oxide phase and corresponds to a diffuse interface approximately 10–15 nm thick [10]. It was also reported [10] that the oxygen and copper concentration profiles vary continuously from the surface to the bulk copper.

The formation of the precursor oxide by thermal treatment is reported for relatively smooth working conditions (i.e., low temperature and short treatment time) and in any cases it takes place before Cu(I) and Cu(II) oxides. Similarly, it is likely that its formation is also favoured by smooth plasma treatments which were limited to a few minutes. After 5 min treatment by the oxygen plasma ($d = 5 \text{ cm}$, $P = 300 \text{ W}$; $P/N = 3.6 \times 10^7 \text{ W mol}^{-1}$) the sample was examined electrochemically. The first reduction sweep exhibits only one minor peak near -0.55 V vs SCE (Fig. 2(a)) which is attributed to the reduction of the precursor oxide. The peak intensity decreases and almost disappears during the second sweep (Fig. 2(b)), which shows that the precursor oxide is nearly completely removed by the first cathodic sweep: this feature also shows that the quantity of precursor oxide laid on the surface by the plasma treatment is very limited.

Since the precursor oxide can be prepared by means of a plasma technique, we found it necessary to define the conditions for an improved yield, and undertook two series of experiments corresponding to 5 min treatments. For the first series we varied the electric power P , and the generator was operated at 100, 200 and 300 W, keeping a constant distance $d = 5 \text{ cm}$ between the sample and the first coil (for $P/N = 1.2 \times 10^7$, 2.4×10^7 and $3.6 \times 10^7 \text{ W mol}^{-1}$). The second series was operated at fixed power ($P = 300 \text{ W}$) and at various positions of the target ($d = 5$, 10 and 20 cm; $P/N = 3.6 \times 10^7$, 1.8×10^7 and $0.9 \times 10^7 \text{ W mol}^{-1}$). In both cases the treated samples were electrochemically analysed. Voltammograms relevant to the first series of samples (Fig. 3) show one re-

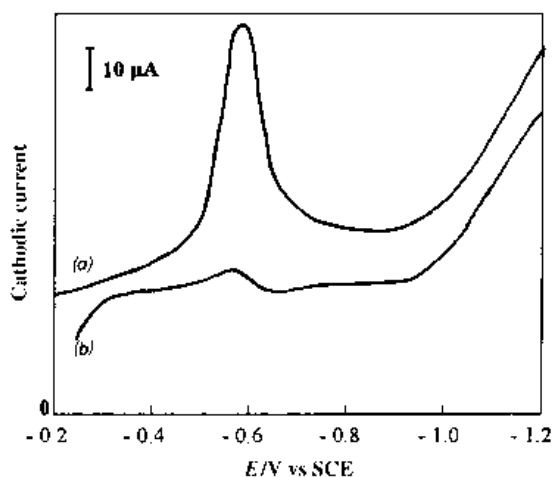


Fig. 2. Cathodic reduction curves of precursor oxide formed by oxygen plasma oxidation of copper foils. (a) First scan; (b) second scan.

duction peak in the range -0.55 ± 0.05 V vs SCE which is attributed to the precursor. The influence of the injected power on the position and the intensity of the reduction peak of the precursor oxide is inferred from these potentiodynamic responses. The peak intensity varies with the injected power P that is with the quantity of oxide formed on the surface, or the thickness of the oxide film. Also for treatments involving more power, the peak potential moves towards more negative values because the composition of the oxide layer is enriched in Cu(I) species [10]. The voltammograms recorded for the second series of experiments illustrate the influence of the distance between the copper target and the first coil at 300 W (Table 2). One reduction peak near -0.55 ± 0.05 V vs SCE is observed, in connection with the reduction of the precursor oxide. The peak intensity increases when the distance decreases, which suggests that the reactivity of the plasma depends directly on d and that, as expected, the plasma treatment is more efficient when the distance to the target is shorter.

The reduction peaks of the Cu(I) oxides layers were intended to identify the Cu_2O and Cu_3O_2 species and for that purpose thin films of various thicknesses were prepared by plasma treatment; their composition was either single Cu_2O oxide or an intimate mixture of Cu_2O and Cu_3O_2 .

Cu_2O prepared by a 15 min plasma treatment ($P = 300$ W, $p = 200$ Pa, $d = 20$ cm for $P/N = 0.9 \times 10^7 \text{ W mol}^{-1}$) is identified by the 820 nm emission band on the photoluminescence spectrum (Fig. 4(a)). The relevant electroreduction curve (Fig. 5(a)) shows a minor peak near -0.5 V vs SCE corresponding to the reduction of the precursor oxide (Cu_xO) present on the oxide layer and a major peak near -0.85 V vs SCE attributed to the reduction of Cu_2O .

For more severe treatment conditions (e.g., $P = 300$ W; $p = 200$ Pa, $d = 10$ cm, $t = 10$ min; $P/N = 1.8 \times 10^7 \text{ W mol}^{-1}$), the luminescence spectrum of the sample shows two emission bands at 760 nm (intense) and 820 nm corresponding to Cu_3O_2 and Cu_2O , respectively (Fig. 4(b)). The voltammetric reduction curve shows a peak at -0.5 V vs SCE relevant to the precursor oxide and a prominent peak at -0.85 V vs SCE corresponding to the reduction of the oxide mixture $\text{Cu}_3\text{O}_2 + \text{Cu}_2\text{O}$ (Fig. 5(b)). Thus, the potential linear sweep voltammetry method is unsuitable to characterize each oxide Cu_3O_2 and Cu_2O present on the metal surface.

The voltammograms of plasma prepared Cu(I) oxide films of various thicknesses also show one reduction peak in the range -0.85 to -1 V vs SCE. Other

Table 2. Influence of the distance on the position and the intensity of the electroreduction peak of the precursor oxide

Distance/cm	5	10	20
$P/N/\text{W mol}^{-1}$	3.6×10^7	1.8×10^7	0.9×10^7
E_p vs SCE/V	-0.58	-0.55	-0.50
$I_p/\mu\text{A}$	-70	-60	-35

$t = 5$ min, $P = 300$ W.

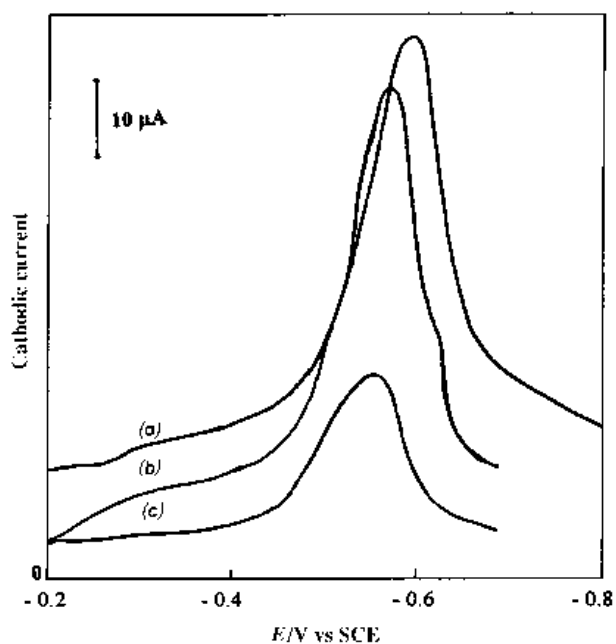


Fig. 3. Cathodic reduction curves of precursor oxides formed by oxygen plasma oxidation of copper foils at different injected powers and at fixed distance ($d = 5$ cm) during 5 min. (a) 300 W, (b) 200 W, (c) 100 W.

authors [11, 31, 32] confirmed that the peak potential depends on the layer thickness and moves towards more negative potentials as the thickness increases. The displacement with immersion time of the peak position in the same range of potentials was also observed by Millet [33] for the reduction of Cu(I) oxides formed after immersion of copper samples in NaCl (0.5 M) solution and attributed [33] to the conduction change of the oxide layer and to an increased quantity of Cu_2O formed on the surface.

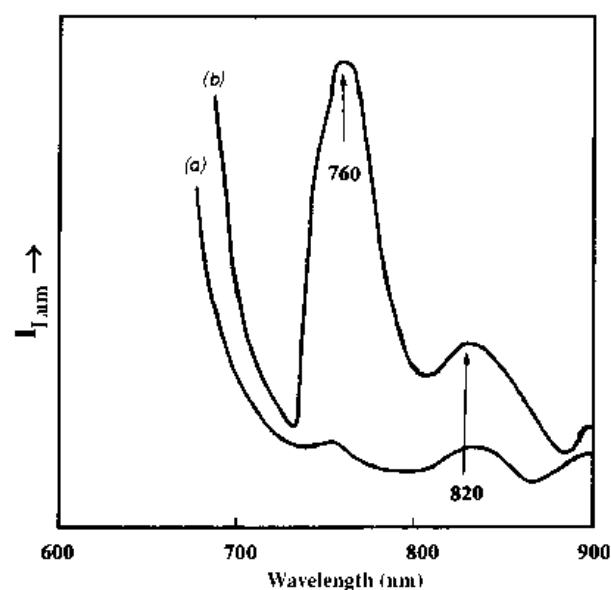


Fig. 4. Emission photoluminescence spectra ($\lambda_{\text{exc}} = 530$ nm) of copper oxidized in oxygen plasma. (a) $P = 300$ W, $p = 200$ Pa, $d = 20$ cm, $t = 15$ min. (b) $P = 300$ W, $p = 200$ Pa, $d = 10$ cm, $t = 10$ min.

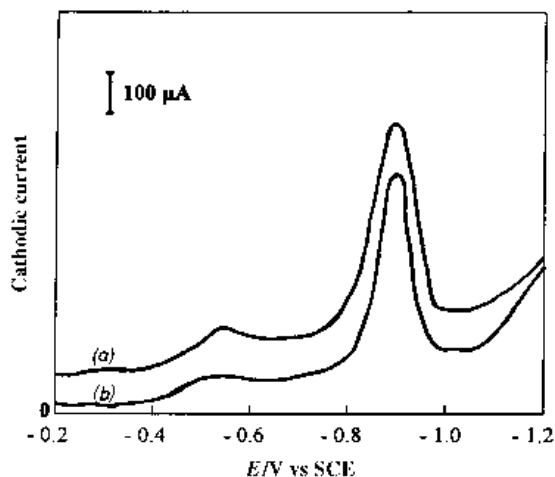


Fig. 5. Cathodic reduction curves of copper(I) oxides formed by oxygen plasma oxidation of copper foils. (a) Cu_2O ; (b) Cu_2O and Cu_3O_2 .

The presence of one copper vacancy per cell in Cu_3O_2 does not result in a change in the reduction peak position of the Cu(I) cations present in Cu_3O_2 . The reduction potential depends only on the quantity of Cu(I) cations in the oxide layer. For this reason, in spite of the fact that Cu_xO may be considered as a structural form of Cu_2O , the precursor oxide was reduced before the two copper(I) oxides. The precursor oxide is less stable than Cu_2O and Cu_3O_2 because it is formed with an intimate mixture of Cu(I) and Cu(0) [10].

The reported electrochemical results relevant to Cu_xO , as well as to Cu_3O_2 and Cu_2O , may be summarized as follows and interpreted in terms of solution electrochemistry: (i) the basic process involved in all cases is the reduction of Cu(I) to metallic copper; and (ii) the reduction peak potential of Cu(I) moves toward more negative potentials, that is Cu(I) becomes more difficult to reduce, as the thickness of the oxide layer or the ratio O/Cu increase. The electrochemical behaviour of Cu(I) is thus very similar to that of a metal cation reduced in solution in the presence of increasing concentrations of complexing agent. In the present case, the oxide layer may be identified as the diffusion layer.

According to this model, which can be developed in terms of activities, the structural effect (e.g., the presence of one copper vacancy per cell in Cu_3O_2) is not directly responsible for the decrease of the reduction peak potential which may better be related to the decrease of the Cu(I) activity in the oxide layer as the oxide enriches in oxygen (or the layer thickness increases).

3.2. Copper(II) oxide

The highest usual oxidation state of copper, (i.e., Cu(II)), could be expected as the result of the Cu(I) oxidation. The optical analysis of CuO is reported [8, 10]. The infrared reflectance spectrum of the CuO/Cu system consists of many bands around 605, 530,

470 cm^{-1} (TO mode) and 620, 580, 550 cm^{-1} (LO mode) [29, 30, 34] and the optical spectrum of CuO is characterized by an abrupt absorption rise in the range 800–900 nm [8, 29, 30].

Severe oxygen plasma treatment leads to the formation of CuO which is the only thermodynamically stable phase, as illustrated by long exposures under standard conditions (i.e., $P = 300 \text{ W}$; $p = 200 \text{ Pa}$; $d = 10 \text{ cm}$; $P/N = 1.8 \times 10^7 \text{ W mol}^{-1}$). The photoluminescence spectrum of a 15 min treated sample confirms the occurrence of a mixture of Cu_2O and Cu_3O_2 at the metal surface. A subsequent electrochemical investigation (Fig 6) shows a minor precursor peak near -0.5 V vs SCE, two peaks at -0.65 V and -0.75 V vs SCE (shoulder) which are, respectively, assigned to the first and second reduction step of CuO and a major peak at -0.82 V vs SCE which is related to the reduction of the Cu(I) oxides. The two reduction peaks of CuO suggest that the transformation takes place in two steps (i.e., $\text{Cu(II)} + e^- \rightarrow \text{Cu(I)}$ [at -0.7 V] and $\text{Cu(I)} + e^- \rightarrow \text{Cu(0)}$ [at -0.8 V]) in agreement with reported results [7, 8, 35].

This example is typical of the results obtained with improved oxidation conditions: in all the cases, the two Cu(I) oxides were formed and the voltammograms showed a single reduction peak for Cu_2O and Cu_3O_2 and a couple of peaks for that of CuO , in addition to the precursor signal. For more severe plasma treatments (i.e., higher injected power, and/or longer exposure time) this precursor signal becomes negligible compared to the reduction peak of the Cu(I) oxides because the precursor oxide practically disappears at the copper metallic surface.

In addition, the discrepancy observed for the reduction of Cu(II) (i.e., the second reduction steps of CuO and the reduction of Cu(I) oxides, respectively, -0.8 V and -0.85 V vs SCE) may be related to the

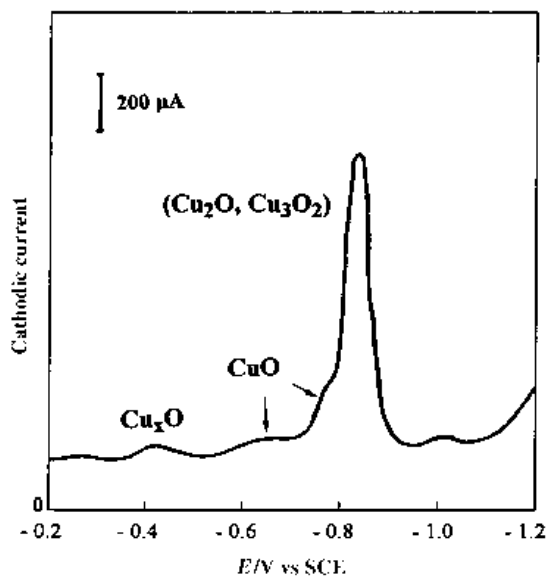


Fig. 6. Cathodic reduction curve of cupric oxide formed by oxygen plasma oxidation of copper foils (injected power = 300 W, pressure = 200 Pa, distance = 10 cm, $P/N = 1.8 \times 10^7 \text{ W mol}^{-1}$).

Table 3. Synopsis of the electrochemical characteristics of the copper oxides

Nature of copper oxide	Precursor oxide	Copper(I) oxides*	Cupric oxide
Peak position on voltammograms: E_p vs SCE/V	$\text{Cu(I)} + e^- \rightarrow \text{Cu(0)}$ -0.55 ± 0.05	$\text{Cu(I)} + e^- \rightarrow \text{Cu(0)}$ $-0.85-1$	$\text{Cu(II)} + e^- \rightarrow \text{Cu(I)}$ -0.65 ± 0.05 $\text{Cu(I)} + e^- \rightarrow \text{Cu(0)}$ -0.80

* Cu(I) : Cu_2O , Cu_3O_2 .

Table 4. Electrochemical analysis of the copper oxides formed by oxygen plasma

Samples treated at 300W during:	5 min	10 min	15 min
Nature of oxide and E_p vs SCE/V	Cu_xO -0.58	Cu_xO -0.5 Cu_2O , Cu_3O_2 -0.90 CuO $\left\{ \begin{array}{l} -0.65 \\ -0.80 \end{array} \right.$	Cu_2O , Cu_3O_2 -1 CuO -1

 $P = 300 \text{ W}$, $p = 200 \text{ Pa}$, $d = 5 \text{ cm}$: $P/N = 3.6 \times 10^7 \text{ W mol}^{-1}$

origin of the species or to differences in hydration as suggested by Deutscher and Woods [7].

In conclusion, the electrochemical reduction of copper oxides in complex layers gives rise to the reactions reported in Table 3. Our results are in excellent agreement with those cited in [7, 8] but disagree with the conclusions of Pops and Hennesy [12] since these authors mistook CuO for Cu_2O in their study of the reduction of oxide layers formed on copper wires.

3.3. Influence of the working parameters

This study shows that the copper oxides formed by plasma treatment can be identified by linear potential sweep voltammetry, except the Cu(I) oxides Cu_2O and Cu_3O_2 that cannot be separated. This technique is, however, convenient to analyse complex oxide films and gather data on the kinetics of the formation of the layers in relation to the plasma standard working conditions mentioned above. The intensity

and the position of the reduction peaks of the different copper oxides depend on the film thickness.

In this Section we emphasize the influence of the discharge parameters on the oxidation kinetics and especially on the exposure time and on the distance between the copper target and the first inductive coil.

The influence of the exposure time is summarized (Table 4) for given conditions: injected electric power, $P = 300 \text{ W}$; gas pressure, $p = 200 \text{ Pa}$; distance, $d = 5 \text{ cm}$; $P/N = 3.6 \times 10^7 \text{ W mol}^{-1}$ which also reports the peak potentials and the nature of the species formed. In all the voltammograms (Fig. 7), the first minor peak near -0.5 V vs SCE is attributed to the precursor Cu_xO (Fig. 7(a), $t = 5 \text{ min}$), the major peak in the range -0.8 to -0.9 V vs SCE to the reduction of Cu(I) [$\text{Cu(I)} + e^- \rightarrow \text{Cu(0)}$] in the Cu(I) oxides (Fig. 7(b), $t = 10 \text{ min}$) while the peaks at -0.65 V vs SCE and -0.80 V vs SCE are, respectively, assigned to the first and second reduction step of CuO. In Figure 7(c) ($t = 15 \text{ min}$) only one major peak at -1 V vs SCE is observed corresponding to the reduction of all the copper oxides formed at the metal

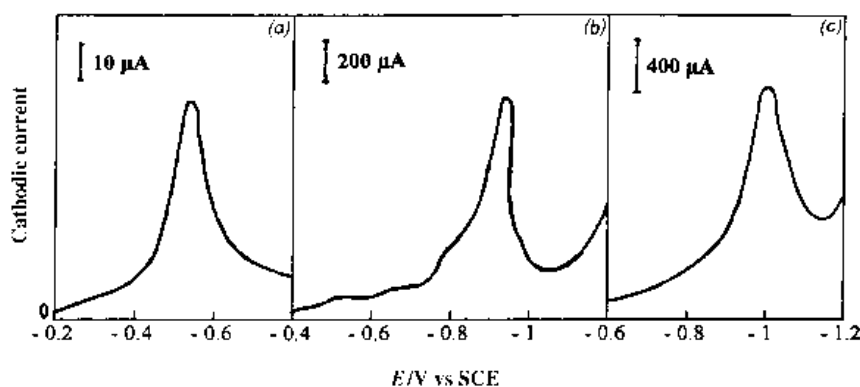


Fig. 7. Cathodic reduction curves of copper oxides formed by oxygen plasma oxidation of copper foils for different exposures (injected power = 300 W, pressure = 200 Pa, distance = 5 cm, $P/N = 3.6 \times 10^7 \text{ W mol}^{-1}$). (a) 5 mn, (b) 10 mn, (c) 15 mn.

Table 5. Influence of the distance on the nature of the oxide formed by oxygen plasma treatment

Samples treated during:	5 min	10 min	15 min	20 min	25 min	30 min	
Oxide formed	$d = 5 \text{ cm}^*$	Cu_xO	$\text{Cu}_x\text{O}, \text{Cu(I)}$ CuO	Cu_2O CuO	CuO		
	$d = 10 \text{ cm}^\dagger$	Cu_xO	$\text{Cu}_x\text{O}, \text{Cu(I)}$	$\text{Cu(I)}, \text{CuO}$	$\text{Cu}_2\text{O}, \text{CuO}$	CuO	
	$d = 20 \text{ cm}^\ddagger$	Cu_xO	$\text{Cu}_x\text{O}, \text{Cu(I)}$	Cu_2O	$\text{Cu}_2\text{O}, \text{CuO}$	$\text{Cu}_2\text{O}, \text{CuO}$	CuO
Film thickness	$d = 5 \text{ cm}^*$	0.17	0.42	0.83	1.2		
	$d = 10 \text{ cm}^\dagger$	0.15	0.18	0.37	0.74	1.20	
	$d = 20 \text{ cm}^\ddagger$	<0.05	0.05	0.30	0.50	0.71	1.05

$P = 300 \text{ W}$, $p = 200 \text{ Pa}$

$\text{Cu(I)}: \text{Cu}_2\text{O}, \text{Cu}_3\text{O}_2$

* $P/N = 3.6 \times 10^7 \text{ W mol}^{-1}$

† $P/N = 1.8 \times 10^7 \text{ W mol}^{-1}$

‡ $P/N = 0.9 \times 10^7 \text{ W mol}^{-1}$

surface (i.e., a thin layer of Cu(I) oxides and a thick CuO film which is evidenced by the black colour of the sample). A single reduction peak is observed for film thickness larger than $0.5 \mu\text{m}$ because the second reduction peak of CuO is masked by the reduction peak of the Cu(I) oxides [8]. This change in the recorded voltammograms is considered by different authors to arise from restructuring of the copper(I) oxides layer, which makes Cu(I) more difficult to reduce [7, 14]. Thus, whereas the initial oxide Cu_xO is reduced close to the reversible potential (-0.5 V vs SCE), a significant overpotential is required to reduce the more stable oxides: Cu(I) and Cu(II) oxides [7, 14]. This explains the increasingly negative reduction potentials for the oxides with increasing oxidation state.

As shown by the results given in Table 5 the nature of the oxides formed depends strongly on the plasma density P/N as well as the thickness of the films determined by interferometry. For short exposures ($t = 5 \text{ min}$) only the precursor oxide is detected. For longer exposures (i.e., 15 min or more) the Cu(II) oxide forms alone or as a mixture with Cu(I) oxides. In all cases the layer thickness is a decreasing function of d (and an increasing function of t). However, at film thickness near $1.2 \mu\text{m}$ and above the oxide layer separates, which provides a practical limit to this process. The layer copper oxide protrudes, probably because the outermost layer was CuO.

4. Conclusions

Cathodic reduction can be used to identify the different oxides formed on a copper surface after exposure to an oxygen plasma under various conditions. The voltammograms of the thin films formed show that the plasma oxidation of the metal takes place in several steps: a precursor oxide Cu_xO ($x > 4$) forms first, followed by an intimate mixture of copper(I) oxides ($\text{Cu}_2\text{O}, \text{Cu}_3\text{O}_2$). The oxidation process ends with the formation of CuO. This work shows that the precursor oxide is the only species formed at the surface after treatment for short exposure times. The reduction potentials of the Cu(I) and Cu(II) oxides vary with the layer thickness. The

reduction of CuO involves two steps and takes place at less negative potentials than that of Cu_2O and Cu_3O_2 which cannot be distinguished by their cathodic reduction peaks.

The products yielded by the plasma treatment are the same as those resulting from a low thermal treatment. They form according to the same sequence but for drastically shortened exposures: for example oxide layers of the same thickness ($e = 0.35 \mu\text{m}$) result from a 15 min plasma treatment ($P = 300 \text{ W}$, $d = 10 \text{ cm}$) or from a 60 min during treatment at low temperature ($T = 523 \text{ K}$) [8].

The relevant chemical reactivity of an inductively coupled oxygen plasma remains the puzzling question since only the effects were shown and no information was reported on the species responsible; it can, however, be explained by the occurrence of many oxidizing charged or uncharged species in the discharge, such as O and O^+ [29, 30] as illustrated by emission spectrometry investigations.

Acknowledgement

The authors thank Professor M. Lenglet for his valuable advice and help in recording the spectra.

References

- [1] J. L. Brisset, S. Longchamp, P. Surlbled and M. Vittecoq, Proc 4th International Symposium on High Pressure Low Temperature Plasma Chemistry, Bratislava, Slovakia (1993) p. 117.
- [2] A. Goldman and R. S. Sigmond, *J. Electrochem. Soc.* **132** (1985) 2842.
- [3] M. Carballeira, A. Carballeira and J. Y. Gal, Proceedings of the 14th International Conference on Electric Contacts, Paris, France (1988) p. 239.
- [4] J. Kúdela, V. Sobek, M. Luknárova P. Lukác and J. D. Skalný, *Acta, Physica Univ. Comeniana* **33** (1992) 209.
- [5] B. G. Bagley, L. H. Greene, J. M. Tarascon and G. W. Hull, *Appl. Phys. Lett.* **51** (1987) 622.
- [6] A. Yoshida, H. Tamura, S. Morohashi and S. Hasuo, *ibid.* **55** (1989) 2354.
- [7] R. L. Deutscher and R. Woods, *J. Appl. Electrochem.* **16** (1986) 413.
- [8] M. Lenglet, K. Kartouni and D. Delahaye, *ibid.* **21** (1991) 697.
- [9] J. M. Machefer, M. Lenglet, D. Blavette, A. Menand and A. D' Huysser, 'Structure and Reactivity of Surfaces',

- Elsevier Sciences Publishers B.V., Amsterdam (1989) p. 625.
- [10] B. Lefez, K. Kartouni, M. Lenglet, D. Rönnow and C. G. Ribbing, *Surf. & Interface Anal.* **22** (1994) 451.
- [11] E. Sutter, C. Fiaud and D. Lincot, *Electrochim. Acta* **38** (1993) 1471.
- [12] H. Pops and D. R. Hennessy, *Wire J.* **10** (1977) 50.
- [13] H. Strehblow and B. Titze, *Electrochim. Acta*, **25** (1980) 839.
- [14] M. R. Gennerro de Chialvo, S. L. Marchiano and A. J. Arvia, *J. Appl. Electrochem.* **14** (1984) 165.
- [15] U. R. Evans and A. Miley, *Nature* **139** (1937) 283.
- [16] P. Pascal, *Nouveau Traité de Chimie Minérale III*, Masson, Paris (1957).
- [17] D. Personn and C. Leygraf, *J. Electrochem. Soc.* **140** (1993)1256.
- [18] J. Y. Malvault, J. Lopitiaux, D. Delahaye and M. Lenglet, *J. Appl. Electrochem.* **25** (1995) 841.
- [19] H. Wieder and A. W. Czanderna, *J. Phys. Chem.* **66** (1962) 816.
- [20] E. G. Clarke and A. W. Czanderna, *Surf. Sci.* **49** (1975) 529.
- [21] H. Neumeister and W. Jaenike, *Z. Phys. Chem.* **B108** (1977) 217.
- [22] M. Lenglet and K. Kartouni, *La Revue de Métallurgie-CIT/ Science et Génie des Matériaux* **12** (1993)1637.
- [23] S. Brahms, J. P. Dahl and S. Nikitine, *J. Phys.* **C3-32** (1967) 28.
- [24] P. Marksteiner, P. Blaha and K. Schwarz, *Z. Physik.* **B64** (1986) 119.
- [25] H. Wieder and A. W. Czanderna, *J. Appl. Phys.* **37** (1966) 184.
- [26] J. Bloem, *Phil. Res. Rep.* **13** (1958) 167.
- [27] C. K. Teh and F. L. Weichman, *Can. J. Phys.* **61** (1983) 1423.
- [28] R. G. Greenler, R. R. Rahn and J. P. Schwartz, *J. Catal.* **23** (1971) 42.
- [29] N. Bellakhal, Thèse, Université Paris VI (1995).
- [30] N. Bellakhal, K. Draou, B. Chéron, M. Lenglet and J. L. Brisset, *Proceedings ISPC 12 Minneapolis, USA* (1995) p.1583.
- [31] H. H. Strehblow and B. Titze, *Electrochim. Acta*, **25** (1980) 839.
- [32] S. M. Wilhelm, Y. Tanizawa, C.Y. Liu and N. Hackerman, *Corros. Sci.* **22** (1982) 791.
- [33] B. Millet, Thèse, Université Paris VI (1994).
- [34] E. Beucher, B. Lefez and M. Lenglet, *Phys. Stat. Sol.* **136** (1993)139.
- [35] N. A. Tolstoi and V. A. Bonch-Bruevich, *Sov. Phys. Solid State* **13** (1971)1135.